Chemical Engineering Journal 478 (2023) 147271

Contents lists available at ScienceDirect

Chemical Engineering Journal

journal homepage: www.elsevier.com/locate/cej

Confining monochromophore in dynamic polymer network for multi-stimuli responsive fluorescence-phosphorescence dual-emission

Yi Yu [a,b], Muqing Si [a,b], Wei Lu [a,b,*], Shuangshuang Wu [a,b], Shuxin Wei [a,b], Baoyi Wu [a,b], Xipao Chen [a,c], Weiping Xie [a,c], Tao Chen [a,b,d,*]

[a] Key Laboratory of Marine Materials and Related Technologies, Zhejiang Key Laboratory of Marine Materials and Protective Technologies, Ningbo Institute of Material Technology and Engineering, Chinese Academy of Sciences, Ningbo 315201, China
[b] School of Chemical Sciences, University of Chinese Academy of Sciences, 19A Yuquan Road, Beijing 100049, China
[c] Technology Center, Ningbo Institute of Materials Technology and Engineering Chinese Academy of Sciences, Ningbo 315201, China
[d] College of Material Chemistry and Chemical Engineering, Key Laboratory of Organosilicon Chemistry and Material Technology, Ministry of Education, Hangzhou Normal University, Hangzhou 311121, Zhejiang, People's Republic of China

ARTICLE INFO

Keywords:
Fluorescence-phosphorescence dual-emission
Dynamic polymer network
Bromine-substituted naphthalimide
Stimuli-responsiveness

ABSTRACT

Organic fluorescence-phosphorescence dual-emission materials are attracting broad attention for their wide potential applications in information technology, display media, etc. Most reported organic systems rely on the combination of two or more luminogens that emit different-colored phosphorescence and fluorescence respectively. By contrast, the fluorescence-phosphorescence dual-emission from one single luminogen system are especially appealing, as they can offer many advantages such as improved luminescence stability, simplified fabrication process and excellent reproducibility. Nevertheless, it remains challenging to achieve stimuli-responsive fluorescence-phosphorescence dual-emission in monochromophore-based organic material. Herein, we specially designed one new bromine-substituted naphthalimide molecule and incorporated it into a dynamic carboxyl hydrogen-bonded polyacrylic acid (PAA) network to produce the robust multi-stimuli-responsive fluorescence-phosphorescence dual-emission materials. Detailed studies demonstrated that high-density carboxyl hydrogen-bonded crosslinks play important roles in the achievement of intense phosphorescence by providing a rigid environment and efficient oxygen barrier to stabilize the triplet-excited states. On this basis, responsive fluorescence-phosphorescence dual-emission characteristic was guaranteed to realize interesting luminescence color changes, because many environmental stimuli (e.g., temperature, humidity, or alcohol) were known to dissociate the carboxyl hydrogen-bonded crosslinks. This reported strategy is expected to be universal and promising for the future development of powerful organic fluorescence-phosphorescence dual-emission materials with versatile uses.

1. Introduction

Organic materials with stimuli-responsive fluorescence-phosphorescence dual-emission at room temperature have recently emerged as a new type of smart luminescent materials, and are attracting increasing interest owing to their wide applications in the field of optical sensing, bio-imaging, information technology and display media [1]. However, since the triplet-excited states of most organic materials are sensitive to temperature/oxygen and usually unstable, their phosphorescence emission efficiency is lower than their fluorescence efficiency [2]. As a result, most organic materials usually display visible phosphorescence only after turning off the irradiation light, which makes the reported applications highly dependent on time-resolved imaging technology and largely restricts the development of direct visualization-based applications [3]. Therefore, in order to achieve efficient fluorescence-phosphorescence dual emission, such difficult challenges as oxygen quenching and fast nonradiative decay of the excited triplet states (T_1) at room temperature should be well addressed to control the proportion between T_1 and the excited singlet states (S_1) through delicate material design [4]. One effective strategy is to confine the chromophores in a relatively rigid environment through molecular crystallization [5], incorporation into a molecular cavity [6], or polymer matrix [7]. In this

* Corresponding authors at: Key Laboratory of Marine Materials and Related Technologies, Zhejiang Key Laboratory of Marine Materials and Protective Technologies, Ningbo Institute of Material Technology and Engineering, Chinese Academy of Sciences, Ningbo 315201, China.
E-mail addresses: luwei@nimte.ac.cn (W. Lu), tao.chen@nimte.ac.cn (T. Chen).

https://doi.org/10.1016/j.cej.2023.147271
Received 22 August 2023; Received in revised form 7 November 2023; Accepted 9 November 2023
Available online 10 November 2023

way, molecular motion is largely restricted, and oxygen exposure is also partially blocked, thus activating the phosphorescence emission. Among these approaches, confining luminogens into an amorphous polymer matrix is particularly attractive, because the polymer matrix not only opens the possibility for easy material processability but also leads to flexible fluorescence-phosphorescence dual-emission films with diverse potential uses [8].

So far, a number of fluorescence-phosphorescence dual-emission polymeric materials have been developed by incorporating two or more luminogens that emit different-colored phosphorescence and fluorescence respectively into a polymer matrix [6d,9]. By contrast, the fluorescence-phosphorescence dual-emission from one single luminogen system can offer many advantages, including improved luminescence stability, a simplified fabrication process, and excellent reproducibility. Especially, if such phosphorescence-fluorescence emission ratio could be largely varied in response to external stimuli (e.g., environmental temperature, humidity), the dynamic and reversible luminescence color changes would be envisaged to bring many potential applications such as rewritable display and color-changing paintings. However, despite its potential, the achievement of stimuli-responsive fluorescence-phosphorescence dual-emission in the monochromophore-based organic material still remains a formidable challenge.

Herein, we design one special organic molecule (Bis-BrNpA) containing two bromine-substituted naphthalimide luminogens and assemble it into the dynamic hydrogen-bonded polyacrylic acid (PAA) matrix to produce flexible luminescent film material Bis-BrNpA-PAA (BB-PAA). Intriguingly, although Bis-BrNpA shows only fluorescence in organic solvents, the self-assembled polymer film emits the desired fluorescence-phosphorescence dual-emission in an air atmosphere at room temperature, rather than mere phosphorescence emission. The high-density carboxyl hydrogen-bonded (H-bonded) crosslinks in the BB-PAA film material are believed to account for the observed fluorescence-phosphorescence dual-emission by providing a rigid environment and efficient oxygen barrier. Importantly, owing to the dynamic nature of H-bonded crosslinks in PAA, the as-prepared BB-PAA film displays reversible phosphorescence-to-fluorescence conversion and thus emission color changes in response to multiple environmental stimuli such as temperature, humidity, or alcohol. Importantly, this proposed strategy has been proved to be generally applicable to realize efficient room temperature fluorescence-phosphorescence dual emission in a series of other dynamic hydrogen-bonded polymeric materials (e.g., poly (2-hydroxyethyl methacrylate) and polyvinyl alcohol). Such monochromophore-based polymer systems with both fluorescence-phosphorescence dual-emission and multi-stimuli responsive luminescence color changes have been seldomly reported, but are highly appealing. Their potential applications for rewritable information display and color-changing paintings are further exploited (Scheme 1).

2. Materials and methods

2.1. Materials

Methanol (MeOH, 99%), ethyl alcohol (EtOH, 99%), and dimethyl formamide (DMF, 99%) were purchased from Sinopharm Chemical Reagent Co. Ltd. Dimethyl sulfoxide (DMSO, 99%), tetrahydrofuran (THF, 99%), ethylene glycol (EG, 99%), sodium bromide (K_2SO_4, 99%), lithium chloride (LiCl, 98%), sodium carbonate (Na_2CO_3, 99%), polyacrylic acid (PAA, M_w: 4.5×10^5 g·mol^{-1}) and 2-hydroxyethylmethacrylate (HEMA, 99%, stabilized with MEHQ) were obtained from Aladdin Chemistry Co. Ltd. 4-Bromo-1,8-naphthalic anhydride (97%) was provided by Alfa Aesar Chemical Co. Ltd. Polyvinyl alcohol (M_w: 1.7×10^3 g·mol^{-1}) was gotten from Energy Chemical. 2,2′-azoisobutyronitrile (AIBN, 99%) was provided by J&K Scientific Ltd. 1,4-butylenediamine (98%) was supplied by Shanghai Macklin Biochemical Co. Ltd. AIBN was purified by recrystallization, and vacuum distillation. HEMA passed through an alumina column to remove the stabilizer before use. Other materials were used without further purification.

2.2. Synthesis of Bis-BrNpA

4-butylenediamine (0.503 mL, 0.005 mol) was added to a suspension of 4-bromo-1,8-naphthalic anhydride (3.048 g, 0.011 mol) in 120 mL of

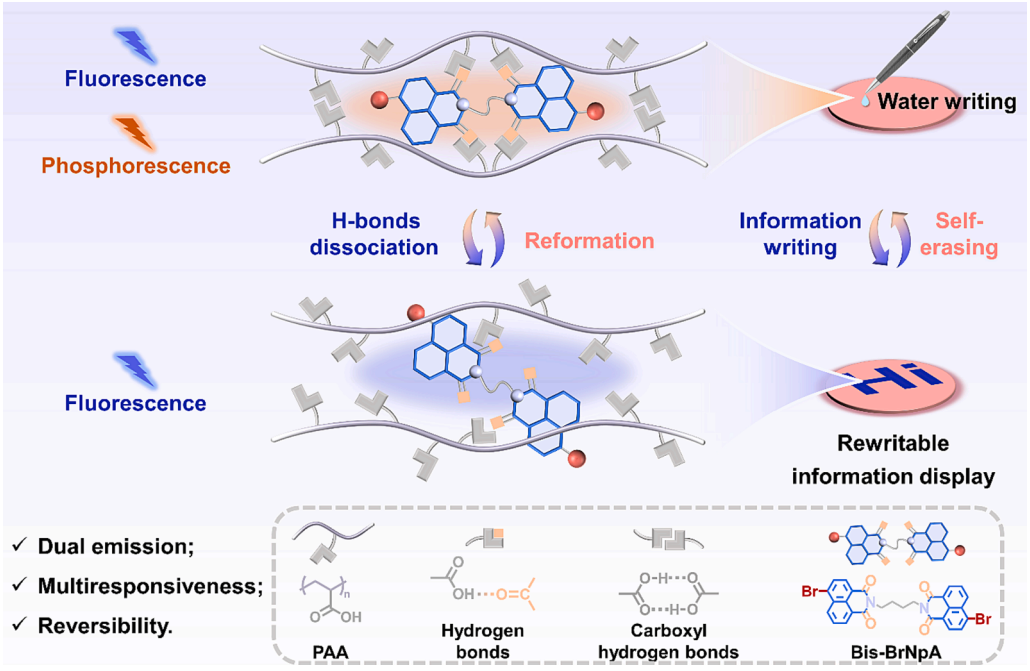

Scheme 1. Schematic illustration showing the responsive fluorescence-phosphorescence dual-emission of thin polymeric film (BB-PAA) for rewritable information display. The PAA matrix provides tunable oxygen barrier property and a rigid environment that serves to stabilize the triplet state of the organic molecule Bis-BrNpA. Meanwhile, the dynamic nature of the H-bonded crosslinks in PAA endows the film with responsive and reversible luminescence color change to enable rewritable information display.

absolute ethanol. The mixture was kept stirring and heated at reflux for 8 h. After the reaction mixture was cooled to room temperature, the precipitate was filtered to get the crude product. Then the crude product was washed with 500 mL saturated Na_2CO_3 aqueous solution and filtered again, afterward dried in a vacuum for 24 h to obtain Bis-BrNpA (3.0215 g, 93%) as a slightly yellow solid. ^{1}H NMR (400 MHz, $CDCl_3$) δ 8.62 (d, $J = 7.2$ Hz, 2H), 8.56 (d, $J = 8.6$ Hz, 2H), 8.38 (d, $J = 7.8$ Hz, 2H), 8.02 (d, $J = 7.9$ Hz, 2H), 7.83 (t, $J = 7.9$ Hz, 2H), 4.25 (t, 4H), 1.88 (m, 4H). ^{13}C NMR (151 MHz, $CDCl_3$) δ 163.64, 133.27, 132.08, 131.27, 131.09, 130.65, 130.25, 129.06, 128.07, 123.13, 122.27, 40.18, 25.73. HR-ESI-MS: $C_{28}H_{18}Br_2N_2O_4$ for $[M + H]^+$, calculated 606.96, found 606.96.

2.3. Fabrication of BB-PAA film

Bis-BrNpA was first dissolved in methanol at 50 °C for 6 h to prepare a spare solution with a concentration of 1.6647×10^{-4} M. 5.0 g PAA was dissolved in 100 mL of stock solution at room temperature under stirring for 2 h. The concentration of the solution was 0.05 g·mL^{-1}. The methanol solution of PAA (10 mL) and Bis-BrNpA (10 mL) were mixed and then added into Petri dish mold (inner diameter 60 mm). The solvent slowly evaporated at room temperature and polymeric film was obtained.

2.4. Fabrication of BB-PHEMA film

The preparation of BB-PHEMA film was similar to that of BB-PAA film. The methanol solution of PHEMA (10 mL) and Bis-BrNpA (10 mL) were blended. Then they were added into Petri dish mold and the solvent slowly evaporated at room temperature. Finally, the polymeric film was gained.

2.5. Fabrication of BB-PVA film

Mixture of PVA (1.0 g) and Bis-BrNpA (2.8 mg) was first dissolved in the deionized water/ ethylene glycol (EG) mixture (1/1, w/w) at 95 °C. After being entirely dissolved, the solution was cast into glass square mold and then cooled at −20 °C for 20 min. Subsequently the mold was removed to give organohydrogel. The organohydrogel was soaked in deionized water for 48 h to exchange EG with excessive water to get hydrogels. The BB-PVA film was obtained by water evaporating naturally.

2.6. Characterization

^{1}H NMR and ^{13}C NMR spectra of Bis-BrNpA were measured on Bruker Advance AMX-400 spectrometer in $CDCl_3$. ESI-MS spectra were recorded on AB Seciex Triple TOF 4600. UV–Vis absorption and transmittance spectra were tested from a UV–Vis spectrophotometer (Lambda 1050+, Perkin Elmer Co., Ltd.). The digital photos of the polymeric films were taken under a UV lamp (ZF-5, 8 W, 365 nm), and all fluorescent photographs were taken by the same UV lamp using a smartphone (iPhone 12mini). FT-IR spectra were obtained with a Thermo Fisher Scientific Nicolet 6700 FT-IR spectrometer with 32 scans, spanning a spectral range of 4000–800 cm^{-1} with a resolution of 4.0 cm^{-1}. Raman scattering characterizations were taken by a Raman system (in Via-reflex, Renishaw) with a 785 nm excitation wavelength. The cross-section morphology of the film was performed by field-emission scanning electron microscopy (SEM, S-4800, Hitachi) with an accelerating voltage of 5.0 kV. Steady-state photoluminescence spectra and time-resolved emission spectra were performed with a Horiba FL3-111 fluorescence spectrofluorometer with a 400 nm long wave pass (LWP) filter at room temperature with a 450 W Xenon lamp, delay time (0.05 ms), flash count (40), time per flash (30 ms). Temperature-dependent delayed emission spectra were obtained by the same spectrofluorometer but equipped with a temperature controller. The photoluminescence quantum yields were measured by Otsuka Photal Electronics QE-2100 Quantum Efficiency Tester and the excitation wavelength was 365 nm. The lifetime (τ) of the emission was determined by fitting the decay curve with a multiexponential decay function:

$$I(t) = \sum_i A_i e^{-\frac{t}{\tau_i}}$$

where A_i and τ_i represent the amplitude and lifetime of an individual component for multiexponential decay profiles, respectively.

The average lifetimes were calculated according to the following equation:

$$\tau_{avg} = \sum \alpha_i \tau_i^2 / \alpha_i \tau_i$$

All DFT calculations were performed using the Gaussian 16 software package. The optimized geometries of the Bis-BrNpA molecule and the corresponding HOMOs and LUMOs were performed at B3LYP/def2tzvp. The solvent effect was considered by the continuum solvent model. The S_0 to S_1, S_0 to T_1 vertical transitions were obtained through TD-DFT using PBE1PBE/def2tzvp.

3. Results and discussion

3.1. Synthesis and photophysical properties of Bis-BrNpA

The luminescent molecule (Bis-BrNpA) as the organic chromophore (Fig. 1a) was conveniently synthesized by one-step condensation reaction of 4-bromo-1,8-naphthalic anhydride and 1,4-butylenediamine in ethanol at elevated temperature (Fig. S1) [10]. Its molecular structure was clearly characterized by ^{1}H and ^{13}C NMR spectra, Fourier Transform Infrared (FT-IR) spectroscopy and ESI-MS spectrum (Fig. S2–S5). The typical ^{1}H signals around 1.8 and 4.3 ppm (methylene hydrogen) and multiple peaks at 7.8 ~ 8.7 ppm (naphthalene ring hydrogen), as well as the ^{13}C signals at 163.6 ppm (carbonyl carbon), 25.7, and 40.2 ppm (methylene carbon) clearly indicated the synthesis of Bis-BrNpA.

The photophysical properties of Bis-BrNpA were then systematically studied in solution. Fig. 1b, c depicted its UV–Vis and steady-state photoluminescence (PL) spectra in various solvents (2×10^{-5} M). Its absorption spectra are quite similar in THF, DMF, and DMSO solution, which show two absorption bands around 342 nm and 356 nm that are ascribed to the π–π^* transition of the bromine-substituted naphthalimide luminogen [11]. The gradual increase in polarity of solvents, including THF ($\lambda_{ab} = 340$ nm), DMF ($\lambda_{ab} = 342$ nm), and DMSO ($\lambda_{ab} = 344$ nm), leads to a redshift (~ 4 nm) of their maximum absorption peaks. Even though the polarity of MeOH is not the biggest among the selected solvents, the longer wavelength absorption with elevated baseline in MeOH solution is observed, which is ascribed to the Mie or light scattering effects as MeOH is a poor solvent and tends to induce the aggregation of Bis-BrNpA molecules [12]. As for the luminescent spectra measurement, the excitation wavelength of 320 nm was chosen because the Bis-BrNpA molecule has intense light absorption at this wavelength range. As shown in Fig. 1c, its THF solution exhibited one single emission band around 389 nm, while noticeable redshifts (~ 9 nm) were observed in the emission spectra of its DMSO solution. As expected, a more evident red shift was observed for its MeOH solution. These results suggested that their luminescence spectra show an obvious dependence on solvent polarity. Similar solvent-dependent photoluminescence behavior was observed at a lower-concentration solution (Fig. S6). This is possibly because the Bis-BrNpA molecule has intramolecular charge transfer (ICT) owing to the presence of an electron-withdrawing Br atom [13], thereby inducing the fluorescence emission. To better understand the inherent ICT transition of the Bis-BrNpA molecule, density functional theory (DFT) calculations were then conducted [14]. As illustrated in Fig. 1d, the electron cloud is localized around the whole bromine-substituted naphthalimide luminogens at its highest occupied

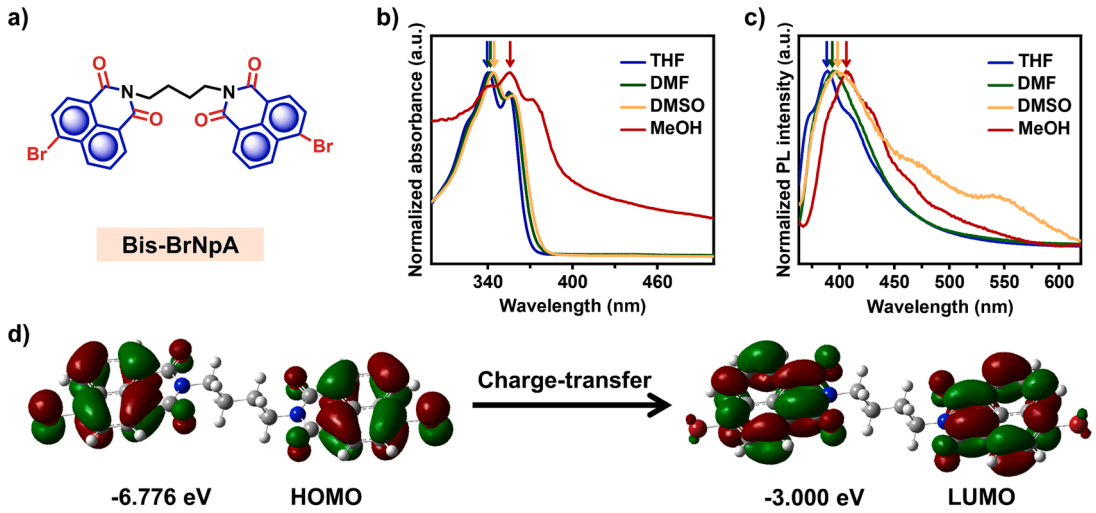

Fig. 1. Molecular structure of Bis-BrNpA and its photophysical properties. a) Chemical structure of Bis-BrNpA. b) Normalized absorbance spectra of Bis-BrNpA in various organic solvents (2×10^{-5} M). c) Normalized photoluminescence spectra of Bis-BrNpA in various organic solvents ($\lambda_{ex} = 320$ nm). d) Calculated ground state HOMO/LUMO energy profiles of Bis-BrNpA in DMSO. DFT calculations were performed with B3LYP/def2tzvp using the Gaussian 16 program.

molecular orbital (HOMO) state, while the lowest unoccupied molecular orbital (LUMO) is mainly localized at the two naphthalimide groups, suggesting the possible occurrence of electron transfer from bromo groups to naphthalimide groups when Bis-BrNpA molecule was excited.

3.2. Fluorescence-phosphorescence dual emission through the confinement of Bis-BrNpA in dynamic polymer networks

Encouraged by the solvent polarity-dependent luminescent properties of the Bis-BrNpA molecules, we next explored the possibility to confine these luminogens into polymer networks for developing soft luminescent polymer films with tunable emission. Towards this end, polyacrylic acid (PAA) was first chosen as the polymer matrix due to its good film-forming capacity and dynamic hydrogen-bonded (H-bonded) crosslinks. As schemed in Fig. S7 in supporting Information, the thin polymer films (BB-PAA) were prepared by pouring the mixed methanol solution of Bis-BrNpA and PAA (Bis-BrNpA/PAA, weight ratio of 1:500) into a Petri dish mold and then allowing the solvent to slowly evaporate at room temperature. The concentration of Bis-BrNpA in methanol is 1.6647×10^{-4} M (Fig. S8) and at this point, the solution is saturated. During the film-forming process, high-density H-bonded crosslinks were formed between the pendent carboxylic acid groups and the carbonyl

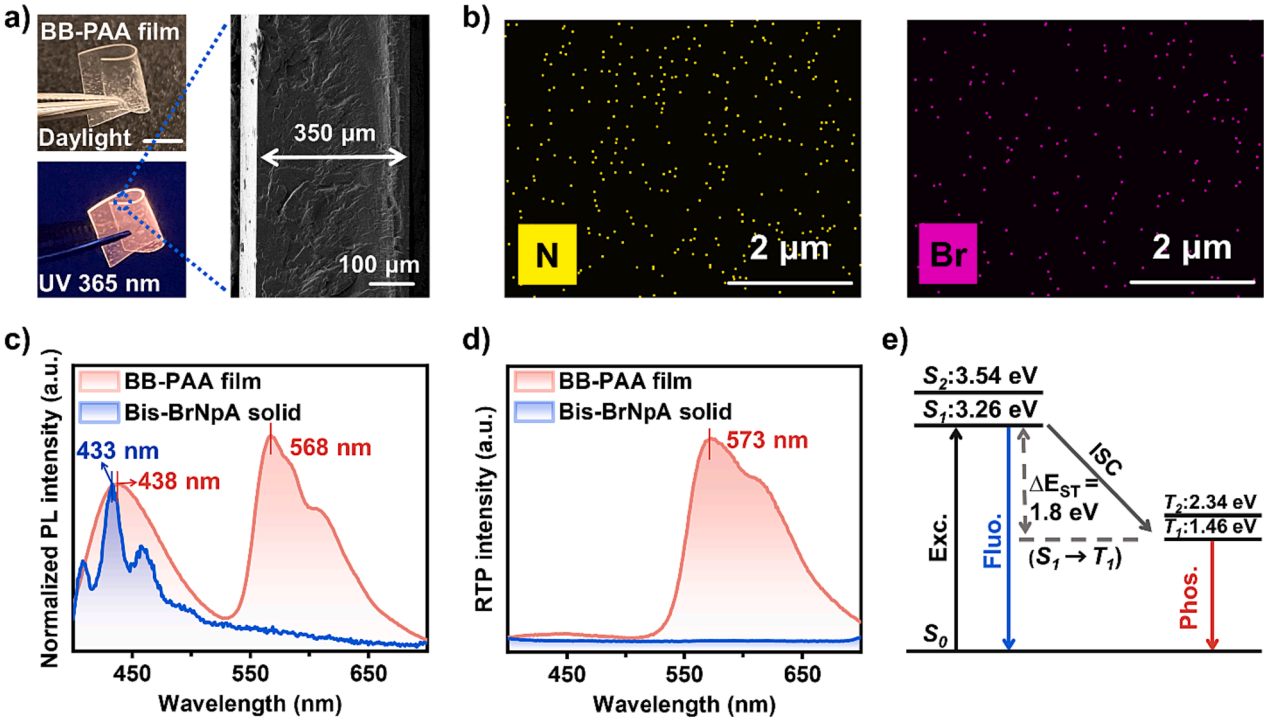

Fig. 2. Fluorescence-phosphorescence dual emission property of the flexible BB-PAA thin film. a) Photographs showing BB-PAA film under daylight, 365 nm UV light (Scale bar is 5 mm), and its SEM image of cross section. b) EDS mapping of N and Br in BB-PAA film. c) Normalized photoluminescence spectra of Bis-BrNpA solid and BB-PAA film. d) The delayed (0.05 ms) photoluminescence spectra of Bis-BrNpA solid and BB-PAA film. e) Calculated energy gaps (eV) between S_1, T_1, and S_0 based on the optimized T_1 geometry for Bis-BrNpA. ($\lambda_{ex} = 365$ nm).

groups of Bis-BrNpA to facilely give the flexible BB-PAA film (Fig. 2a). The as-prepared BB-PAA film (thickness ~ 350 μm, obtained from the scanning electron microscope images, SEM) was highly transparent under daylight with transmittance above 85% at 400 nm (Fig. S9). As shown in Fig. 2b, the results of elemental mapping (for N and Br) by energy-dispersive X-ray spectroscopy (EDS) further indicated the uniform distribution of Bis-BrNpA molecules in the obtained polymer films.

Photophysical properties of the obtained BB-PAA thin film were then systematically studied. Fig. S10 compared its UV–Vis spectra and that of the pure Bis-BrNpA solid. They showed similar absorption behaviors. In consistency with the high transparency under daylight, no evident absorption band of the film was observed in the visible region. As shown in Fig. S10, the primary absorption band was centered at 347 nm, which was significantly redshifted compared with that of the Bis-BrNpA molecule recorded in dilute THF solution (~ 340 nm, THF is a good solvent for Bis-BrNpA). Moreover, a red-shifted absorption spectrum was also observed for the MeOH solution of Bis-BrNpA, because MeOH is a bad solvent for Bis-BrNpA and prone to form Bis-BrNpA aggregates. These experimental results suggested that Bis-BrNpA may form aggregates in the obtained BB-PAA film. As shown in Fig. 2c and S11, the Bis-BrNpA solid displayed an emission band centered at 433 nm with nearly negligible photoluminescence quantum yield (0.1%) and very short nanosecond fluorescence lifetime ($\tau_{433\ nm}$ = 11 ns), which should be ascribed to fluorescence rather than thermally activated delayed fluorescence. Fig. S12 showed the photographs of Bis-BrNpA solid under daylight and 365 nm UV light. Astonishingly, not only a red-shifted emission band at 438 nm but also a new emission band at 568 nm was observed in the steady-state photoluminescence spectra of BB-PAA film taken in air at room temperature. The photoluminescence quantum yield of BB-PAA film was 7.2%. To reveal the origination of this new long-wavelength emission, the time-resolved (delayed) photoluminescence spectra (Fig. 2d) obtained 0.05 ms after excitation was recorded, which exhibited only one single emission band at 573 nm. This observation, together with its microsecond lifetime ($\tau_{568\ nm}$ = 6.3 ms) shown in Fig. S13, suggested that this red-shifted emission band around 568 nm should be assigned as phosphorescence, and its phosphorescence quantum yield was calculated to be 5.5%, while the higher-energy emission band at 438 nm with nanosecond lifetime ($\tau_{438\ nm}$ = 20 ns) should originate from fluorescence [1b]. Moreover, the value of the energy gap between S_1 and T_1 (ΔE_{ST}) for the BB-PAA film could be obtained as 1.8 eV according to the time-dependent density functional theory (TD-DFT) calculation. The ΔE_{ST} in the doped film was large enough to block the reverse intersystem crossing for T_1 to S_1, which facilitated the phosphorescence emission (Fig. 2e) [6b,15]. The computational details can be found in the supporting Information for Bis-BrNpA (Fig. S14). Next, the ratio of Bis-BrNpA has a great influence on the phosphorescence/fluorescence emission ratio (defined as $I_{568\ nm}/I_{438\ nm}$) of BB-PAA film. In order to obtain the film possessing stronger emission, we prepared the film containing different weight ratio of Bis-BrNpA (Fig. S15). As shown in Fig. S15, the phosphorescence/fluorescence emission ratio of BB-PAA film was highly dependent on the Bis-BrNpA/PAA weight ratio. It was found that when the Bis-BrNpA/PAA weight ratio was 1:500, the ratio of $I_{568\ nm}/I_{438\ nm}$ reached the maximum. Therefore, the Bis-BrNpA/PAA weight ratio of 1:500 was employed for the studies except as otherwise noted. Compared with the BrNpA doped polymer film (0.5% by weight [13a]), our Bis-BrNpA doped polymer film exhibited intense room-temperature fluorescence phosphorescence dual-emission with a longer lifetime (6.3 ms), possibly because the closer proximity of two BrNpA luminogens in Bis-BrNpA could enable more stable triplet excitons. Interestingly, nearly identical fluorescence and phosphorescence peaks were recorded in air or N_2 atmosphere, suggesting the negligible influence of oxygen (O_2) on the photophysical properties of BB-PAA film (Fig. S16). In this way, the flexible polymer film with unexpected dual-mode luminescence was prepared, which was capable of emitting stable fluorescence and phosphorescence in the air at room temperature.

3.3. Temperature-responsive phosphorescence change and the mechanism

Owing to dynamic H-bonded crosslinks of the PAA matrix, the fluorescence-phosphorescence dual-emission BB-PAA thin film displayed interesting temperature-dependent luminescence spectra. As shown in Fig. 3a, a large phosphorescence reduction (75%) at 568 nm was observed upon raising the temperature from 25 °C to 85 °C, while there was only slight fluorescence intensity loss (23%) at 438 nm. This observation was consistent with the excitation-emission mapping results (Fig. 3b), which showed significant intensity loss of the red phosphorescence at elevated temperature. These results indicated that the phosphorescence intensity of BB-PAA thin film was more sensitive to temperature variations, resulting in noticeable temperature-dependent emission color changes (Fig. S17). Dynamic “color-changing leaves” paint was also demonstrated (Fig. S18, Movie S1) in which these red leaves quickly turned to be purplish at an elevated environment temperature. To gain insight into the detailed molecular interactions in BB-PAA film for such luminescence responses, variable-temperature FT-IR spectroscopy was conducted. As shown in Fig. 3c, upon temperature elevation from 23 to 95 °C, the signal around 1750 cm^{-1} (free C=O) gradually increased, and meanwhile, the signal around 1660 cm^{-1} (H-bonded C=O) decreased, indicating the dissociation of H-bonded interactions [16]. Another prominent absorption band (attributed to the O–H stretch) was centered around 3100 cm^{-1} and extending approximately from 2800 cm^{-1} to 3400 cm^{-1} mainly due to the strong intermolecular H-bonding interactions of the pendant carboxylic acids [17]. As can be seen from Fig. 3c below, its signal intensity gradually decreased with increasing temperature, indicating the weakening of these intermolecular H-bonding interactions. As a powerful tool for extracting more subtle spectral information, two-dimensional correlation spectroscopy (2DCOS) analysis was carried out to discern the sequential thermal response of different species (Fig. 3d) [18]. The response order of these peaks was speculated as follows: ν (3100 cm^{-1}) → ν (1660 cm^{-1}) → ν (1750 cm^{-1}). According to Noda’s judging rule [19], these results suggested that with increasing temperature, the O-H moieties moved first to dissociate the H-bonds with C=O groups. On the basis of these findings, the microscopic molecular mechanism for such temperature-dependent fluorescence-phosphorescence responses of BB-PAA thin film could be speculated and schemed in Fig. 3e. At room temperature, the Bis-BrNpA molecules were firmly incorporated in the H-bonded PAA network, which provided a rigid environment and oxygen protection to activate efficient room-temperature phosphorescence. At elevated temperature, these H-bonded interactions were gradually dissociated to enable fast nonradiative decay and oxygen quenching, resulting in noticeable luminescence spectral change. After returning to room temperature, H-bonded polymer network was reformed to recover the phosphorescence (Fig. S19).

3.4. Multi-stimuli responsiveness

Having demonstrated that the dynamic H-bonded polymer network is essential for the intense phosphorescence of flexible BB-PAA thin film around 568 nm, we next explored the possibility to regulate its emission spectra and color by employing environmental humidity or alcohol vapor that can form strong H-bonds with PAA. To this end, steady-state photoluminescence spectra were recorded at different time intervals after placing the as-prepared BB-PAA thin film in a high-humidity environment (Relative humidity, RH~ 98%). Note that the water solubility of BB-PAA film is very good, water cannot be directly dropped on the film. As summarized in Fig. 4a and S20, the phosphorescence band was found to gradually decrease within tens of minutes, which is attributed to the fact that more water molecules diffuse into the film with time, dissociating the H-bonded PAA network and thus destroying the rigid environment and oxygen protection provided by the PAA network. As a result, humidity-dependent emission color change was visible because there is significant phosphorescence loss for the BB-PAA

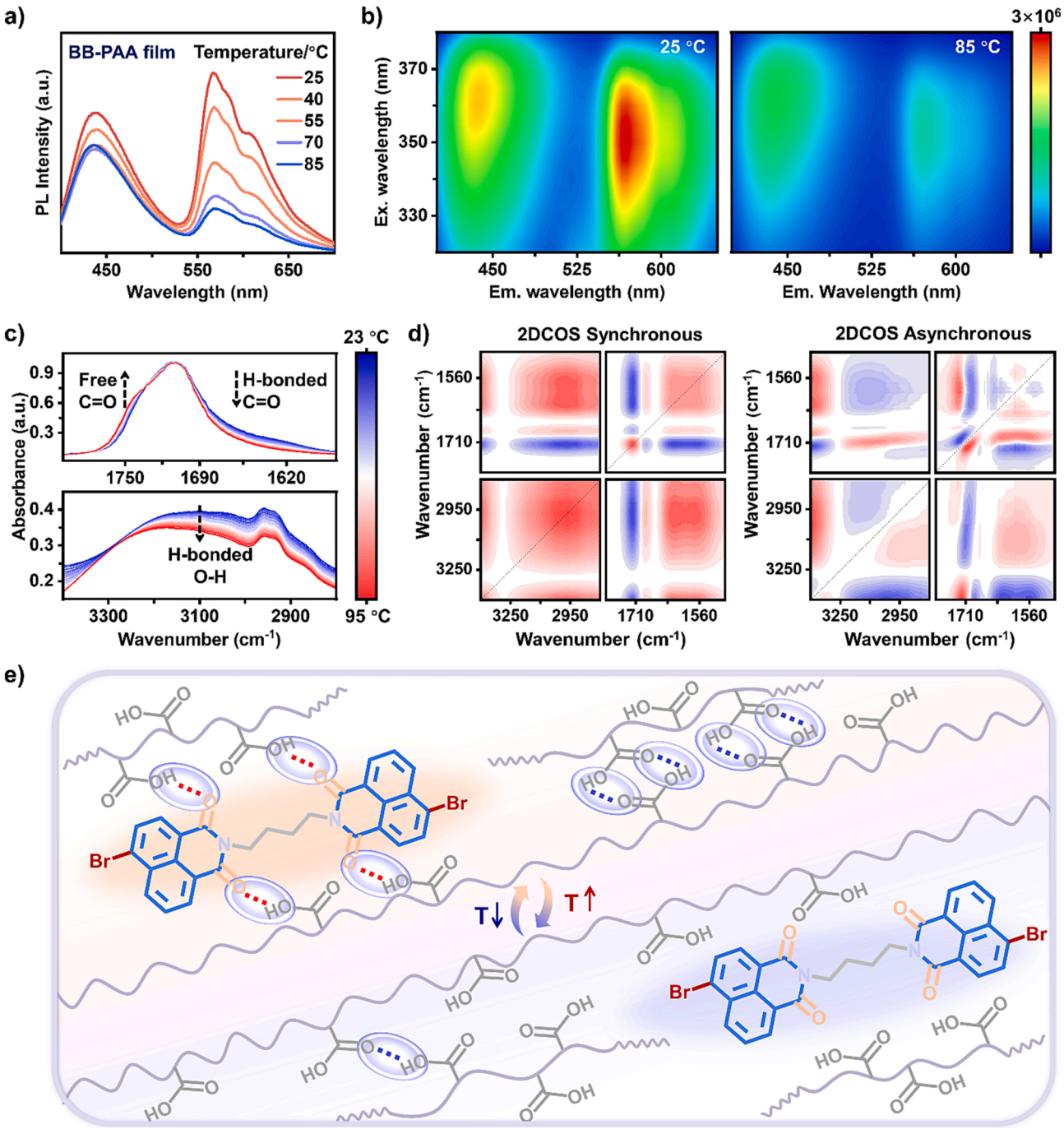

Fig. 3. Temperature-responsive phosphorescence change of the BB-PAA film. a) Steady-state photoluminescence spectra of BB-PAA film measured at 25, 40, 55, 70, and 85 °C. b) Luminescence mapping of BB-PAA film at 25 °C (left) and 85 °C (right). c) Temperature-dependent FT-IR spectra of BB-PAA film upon heating from 23 to 95 °C (interval: 3 °C). d) Two-dimensional COS synchronous and asynchronous spectra wherein red and blue colors are defined as positive and negative intensity, respectively. e) Schematic illustration showing the possible mechanism of the luminescence color variation of BB-PAA film when the temperature changed. (λ_{ex} = 365 nm).

film at high humidity. This observation was consistent with the excitation-emission mapping results (Fig. 4b), which showed significant intensity loss of the red phosphorescence after a long exposure time (30 min). To provide direct evidence for such humidity-triggered phosphorescence change, in-situ Raman mapping of the BB-PAA film surface (Fig. 4c) was conducted, which suggested that a large quantity of water molecules have diffused into the BB-PAA film surface after being placed at RH~ 98% for 30 min to vanish the red phosphorescence [20]. Meanwhile, there was only a relatively small intensity change for the blue fluorescence band, thus leading to environmental humidity-triggered emission color changes (Fig. S21), and the corresponding luminescent photos of BB-PAA were shown in Fig. S22. Interestingly, such humidity-responsive emission response was proved to be highly reversible, as evidenced by the fact that the intense phosphorescence peak could be fully recovered after re-placing the film in a dry atmosphere (RH~ 11%) to trigger the re-formation of H-bonded polymer network (Fig. 4d). Following a similar mechanism, reversible emission color change was also observed for the BB-PAA thin film upon exposure to alcohol vapors such as ethanol. Also, interesting emission color change was noticed under the illumination of different-wavelength

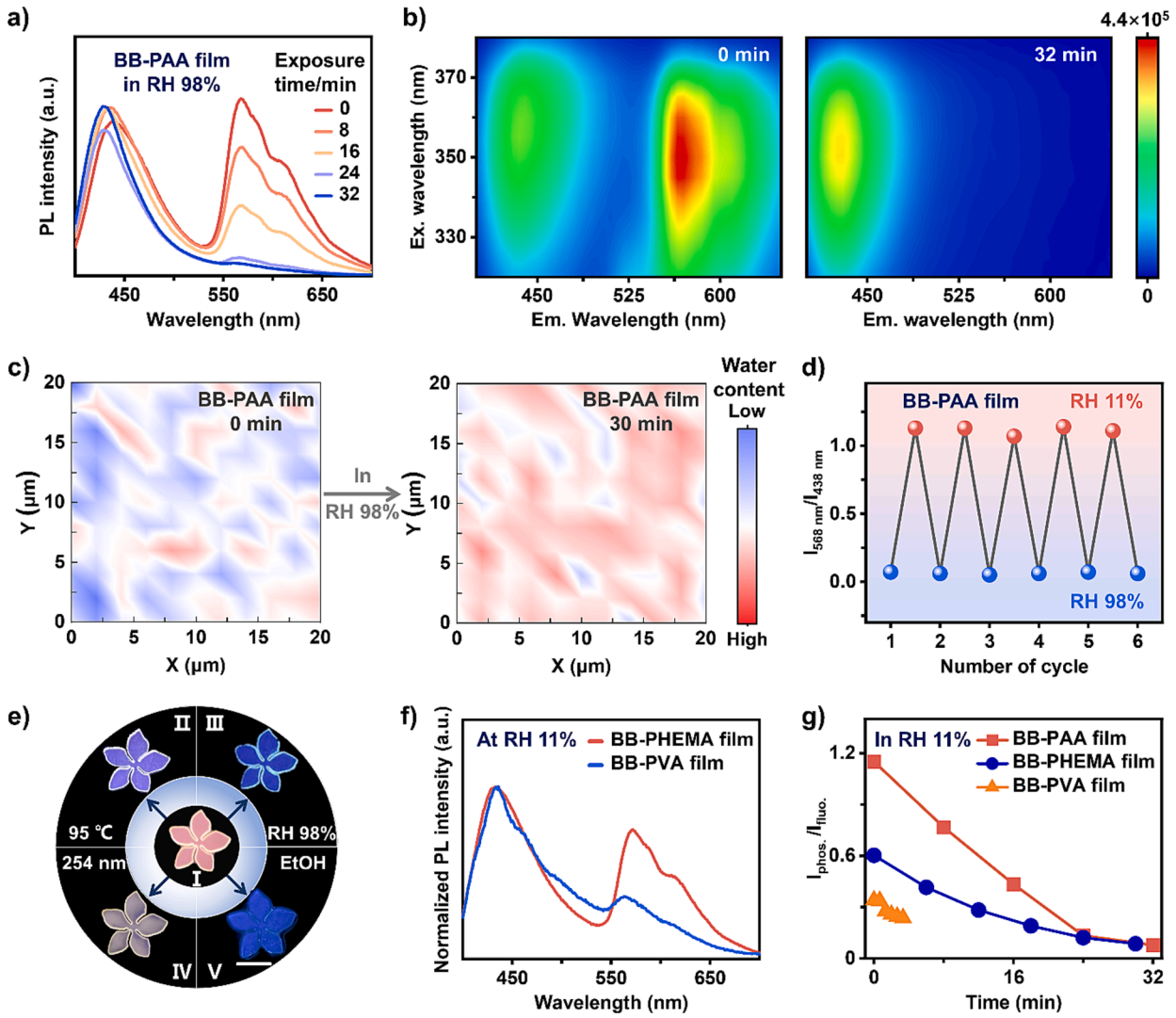

Fig. 4. Multi-stimuli-sensitive luminescence color changes of BB-PAA film and Bis-BrNpA in different polymer matrixes. a) Time-dependent photoluminescence spectra of BB-PAA film recorded in RH~ 98% and b) luminescence mapping of BB-PAA film before and after being placed in RH~ 98% for 32 min. c) Raman mapping of BB-PAA film surface before and after being placed in RH~ 98% for 30 min. The red color means higher water content. d) A plot of the $I_{568\ nm}/I_{438\ nm}$ of BB-PAA film versus the number of cycles by varying the RH between 11 and 98 % alternately. e) Luminescence photos showing the multi-color changes of BB-PAA film in response to multiple environmental changes. I: in RH~ 11%, at 25 °C. Scale bar is 5 mm. All photos were taken under a 365 nm UV lamp. f) Photoluminescence spectra of BB-PHEMA film and BB-PVA film at RH~ 11%. g) Time-dependent $I_{phos.}/I_{fluo.}$ changes of these films after being placed in RH~ 98%. (λ_{ex} = 365 nm).

excitation lights (e.g., from 365 nm to 254 nm), because Bis-BrNpA molecules have strong absorption bands at longer wavelength ranging from 300 nm to 390 nm. Fig. 4e summarized the luminescent images of BB-PAA thin film in response to various environmental stimuli such as temperature, humidity, alcohol, and light.

In the above studies, the fluorescence-phosphorescence dual-emission polymer materials with desired multi-responsive emission color changes have been demonstrated by assembling the organic chromophore (Bis-BrNpA) into a dynamic H-bonded PAA network. Actually, this reported strategy can be generally applicable. As shown in Fig. 4f, the fluorescence-phosphorescence dual-emission polymer films have also been prepared by utilizing poly (2-hydroxyethyl methacrylate) (PHEMA) and polyvinyl alcohol (PVA) bearing plenty of pendant hydroxyl groups as the polymer matrix. The preparation of BB-PHEMA film was similar to that of BB-PAA film, while the fabrication of BB-PVA film was shown in Fig. S23 in supporting information. Both of the films (thickness of BB-PHEMA film ~ 190 μm, BB-PVA film ~ 80 μm, obtained from SEM, Fig. S24) were also highly transparent under daylight (Fig. S25) and flexible (Fig. S26). Compared with that of BB-PAA film, the phosphorescence intensities of BB-PHEMA film and BB-PVA film were relatively small. Such observation could be understood, because the H-bonded polymer networks in BB-PHEMA film and BB-PVA film were formed between the pendant –OH groups, and thus displayed a weaker restriction environment and less efficient oxygen barrier than the carboxyl H-bonded polymer network in BB-PAA film. As expected, these BB-PHEMA film and BB-PVA films also exhibited humidity-responsive emission spectra and color changes (Fig. S27, S28), and the corresponding luminescent photos of BB-PHEMA and BB-PVA were shown in Fig. S29. Nevertheless, the phosphorescence of these polymeric films displayed different sensitivity to humidity (Fig. 4g). In-situ Raman mapping of the films surface (Fig. 4c, S30) demonstrated a large quantity of water molecules have diffused into these films surface to vanish the phosphorescence. As a comparison, the responsive luminescent spectra of Bis-BrNpA solid in response to temperature, humidity, and alcohol have been also conducted and summarized in Fig. S31. In general, luminescent behaviors of the Bis-BrNpA solid were slightly sensitive to temperature, humidity, and ethanol. However, when compared with that of BB-PAA film, BB-PHEMA and BB-PVA film, it was obvious that the Bis-BrNpA solid has only fluorescence emission but almost no phosphorescence emission.

3.5. Responsive luminescence color changes for rewritable or interactive display

The flexible BB-PAA thin film, characterized by multi-responsive dynamic and reversible emission color changes, further encouraged us to explore their intelligent display functions and uses [21]. To show this potential, we first utilized a Petri dish mold to prepare one round-shaped BB-PAA thin film. As shown in Fig. 5a, b, the blue luminescent "Hi" word was capable of being clearly printed on the purplish-red luminescent BB-PAA thin film substrate by using water as the ink, because water has been demonstrated to quench its red phosphorescence. Interestingly, the water-written word would be completely self-erased after being placed in a dry atmosphere (RH~ 11%) to allow the evaporation of water ink and thereby the recovery of red phosphorescence. As a result, another word or pattern could be written on the BB-PAA thin film substrate and subsequently self-erased to enable the re-writing or re-printing of new information. Since the water ink is green and free-of-residue, our flexible BB-PAA thin film holds great potential to serve as an ideal rewritable "paper" to reduce single-use paper consumption.

Besides rewritability, interactive display function could also be guaranteed for the flexible BB-PAA thin film owing to its satisfying environmental humidity-responsive phosphorescence-to-fluorescence conversion nature. Fig. 5c showed a "flowers and leaves" picture example, in which the three "flower" parts were prepared from BB-PAA film, and other parts were made with non-responsive commercial luminescent paint. In a low-RH environment (~ 11%), the flower kept red luminescent. But when the environment RH increased to 98%, time-dependent emission color change would be noticed for these three flowers as an increasing amount of water molecules diffused into BB-PAA film to gradually reduce the red phosphorescence with prolonging time (Movie S2). Other examples showing the humidity-trigged color changing process of "colorful leaves" was presented in Fig. 5d. These leaves were made from two kinds of luminescent polymeric films BB-PAA and BB-PHEMA, which were capable of exhibiting two-stage luminescence color changes because of their differential humidity sensitivity. Similarly, dynamic color-changing "underwater world" paint was also demonstrated in Fig. S32 in supporting Information. In this way, the environment-interactive multicolor display was achieved for our flexible films, suggesting its potential uses for dynamic luminescence-color changeable paints.

4. Conclusion

In summary, a promising approach for producing a new type of luminescent polymeric film is developed by assembling the specially designed bromine-substituted naphthalimide molecules into a dynamic

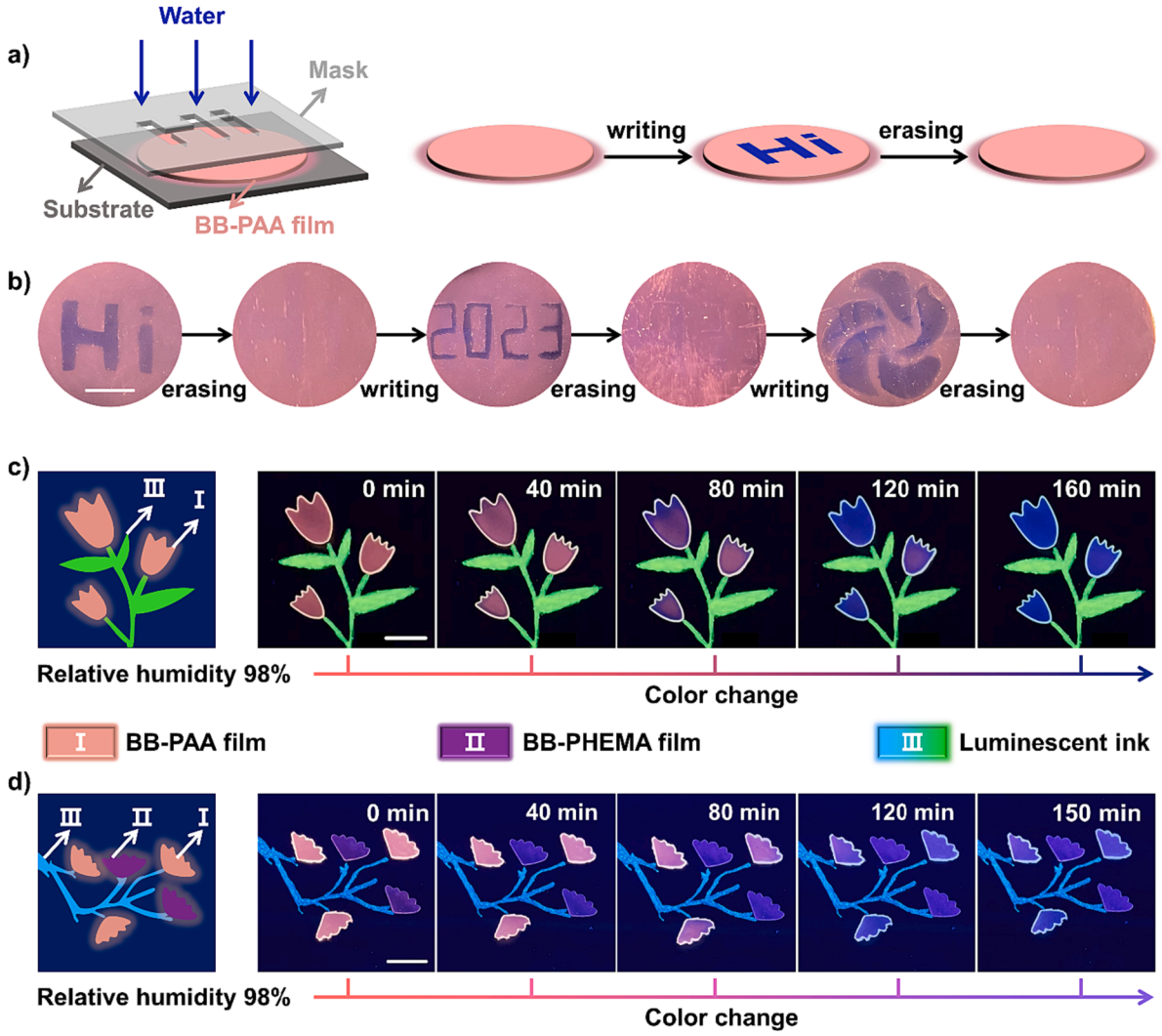

Fig. 5. Rewritable display and environment-interactive color-changing paintings. a) and b) Photos showing the information "writing-erasing-rewriting" process on the BB-PAA film surface by using water as the ink. Photos showing the humidity-trigged color changing process of c) "withering flowers" and d) "colorful leaves" placed in RH~ 98%. All photos were taken under a 365 nm UV lamp. Scale bar is 1 cm.

H-bonded PAA matrix. The obtained monochromophore-based polymeric films show intense phosphorescence and fluorescence dual-emission characteristics and multi-stimuli responsive luminescence color changes. Systematical studies suggest that high-density carboxyl H-bonded crosslinks in the obtained polymeric films play important roles in achieving such phosphorescence-fluorescence dual-emission, which provide rigid environments and efficient oxygen barriers to stabilize triplet excitons. Moreover, the proposed strategy has been demonstrated to be universally applicable for achieving efficient fluorescence and phosphorescence dual emission at room temperature in a range of dynamic hydrogen-bonded polymeric materials, such as PAA, PHEMA, and PVA. Under external stimuli (e.g., environmental temperature and humidity), these carboxyl H-bonded crosslinks are prone to be dissociated to largely vary the phosphorescence-fluorescence emission ratio and thus produce visible luminescence color change, paving the way for rewritable display and color-changing painting applications. Considering the modular design principle of the developed luminescent films, the reported strategy contributes to the development of smart luminescent materials and is expected to be further generalized to fabricate robust phosphorescence-fluorescence dual-emission polymeric films for versatile uses.

Declaration of Competing Interest

The authors declare that they have no known competing financial interests or personal relationships that could have appeared to influence the work reported in this paper.

Data availability

Data will be made available on request.

Acknowledgements

This study was supported by National Natural Science Foundation of China (22322508), the Sino-German mobility programme (M-0424), Zhejiang Provincial Natural Science Foundation of China (LR23E030001), Ningbo Natural Science Foundation (2021J194).

Appendix A. Supplementary data

Supplementary data to this article can be found online at https://doi.org/10.1016/j.cej.2023.147271.

References

[1] a) S. Wang, K. Gu, Z. Guo, C. Yan, T. Yang, Z. Chen, H. Tian, W.H. Zhu, Self-assembly of a monochromophore-based polymer enables unprecedented ratiometric tracing of hypoxia, Adv. Mater. 31 (3) (2019) 1805735, https://doi.org/10.1002/adma.201805735;
b) X.Q. Liu, K. Zhang, J.F. Gao, Y.Z. Chen, C.H. Tung, L.Z. Wu, Monochromophore-based phosphorescence and fluorescence from pure organic assemblies for ratiometric hypoxia detection, Angew. Chem. Int. Ed. 59 (52) (2020) 23456–23460. https://doi.org/10.1002/anie.202007039;
c) Y.Y. Hu, X.Y. Dai, X. Dong, M. Huo, Y. Liu, Generation of tunable ultrastrong white-light emission by activation of a solid supramolecule through bromonaphthylpyridinium polymerization, Angew. Chem. Int. Ed. 61 (44) (2022). https://doi.org/10.1002/ange.202213097;
d) X.Y. Dai, Y.Y. Hu, Y. Sun, M. Huo, X. Dong, Y. Liu, A highly efficient phosphorescence/fluorescence supramolecular switch based on a bromoisoquinoline cascaded assembly in aqueous solution, Adv. Sci. 9 (14) (2022) 2200524, e202213097, https://doi.org/10.1002/advs.202200524.

[2] a) Q. Peng, H. Ma, Z. Shuai, Theory of long-lived room-temperature phosphorescence in organic aggregates, Acc. Chem. Res. 54 (4) (2021) 940–949, https://doi.org/10.1021/acs.accounts.0c00556;
b) W. Zhao, Z. He, B.Z. Tang, Room-temperature phosphorescence from organic aggregates, Nat. Rev. Mater. 5 (12) (2020) 869–885. https://doi.org/10.1038/s41578-020-0223-z;
c) W. Dai, X. Niu, X. Wu, Y. Ren, Y. Zhang, G. Li, H. Su, Y. Lei, J. Xiao, J. Shi, B. Tong, Z. Cai, Y. Dong, Halogen bonding: A new platform for achieving multi-stimuli-responsive persistent phosphorescence, Angew. Chem. Int. Ed. 61 (13) (2022). https://doi.org/10.1002/ange.202200236;
d) X. Ma, J. Wang, H. Tian, Assembling-induced emission: An efficient approach for amorphous metal-free organic emitting materials with room-temperature phosphorescence, Acc. Chem. Res. 52 (3) (2019) 738–748. https://doi.org/10.1021/acs.accounts.8b00620;
e) Z.A. Yan, X. Lin, S. Sun, X. Ma, H. Tian, Activating room-temperature phosphorescence of organic luminophores via external heavy-atom effect and rigidity of ionic polymer matrix, Angew. Chem. Int. Ed. 133 (36) (2021) 19887–19891, e202202692, https://doi.org/10.1002/ange.202108025.

[3] a) S. Sun, J. Wang, L. Ma, X. Ma, H. Tian, A universal strategy for organic fluid phosphorescence materials, Angew. Chem. Int. Ed. 60 (34) (2021) 18557–18560, https://doi.org/10.1002/anie.202107323;
b) W. Dai, Y. Zhang, X. Wu, S. Guo, J. Ma, J. Shi, B. Tong, Z. Cai, H. Xie, Y. Dong, Red-emissive organic room-temperature phosphorescence material for time-resolved luminescence bioimaging, CCS Chem. 4 (8) (2022) 2550–2559. https://doi.org/10.31635/ccschem.021.202101120;
c) Y. Zhou, W. Qin, C. Du, H. Gao, F. Zhu, G. Liang, Long-lived room-temperature phosphorescence for visual and quantitative detection of oxygen, Angew. Chem. Int. Ed. 58 (35) (2019) 12102–12106. https://doi.org/10.1002/anie.201906312.

[4] X. Bi, Y. Shi, T. Peng, S. Yue, F. Wang, L. Zheng, Q.E. Cao, Multi-stimuli responsive and multicolor adjustable pure organic room temperature fluorescence-phosphorescent dual-emission materials, Adv. Funct. Mater. 31 (24) (2021) 2101312, https://doi.org/10.1002/adfm.202101312.

[5] a) F. Nie, B. Zhou, D. Yan, Ultralong room temperature phosphorescence and reversible mechanochromic luminescence in ionic crystals with structural isomerism, Chem. Eng. J. 453 (2023), https://doi.org/10.1016/j.cej.2022.139806;
b) S.M.A. Fateminia, Z. Mao, S. Xu, Z. Yang, Z. Chi, B. Liu, Organic nanocrystals with bright red persistent room-temperature phosphorescence for biological applications, Angew. Chem. Int. Ed. 56 (40) (2017) 12160–12164;
c) W. Qin, J. Ma, Y. Zhou, Q. Hu, Y. Zhou, G. Liang, Simultaneous promotion of efficiency and lifetime of organic phosphorescence for self-referenced temperature sensing, Chem. Eng. J. 400 (2023);
d) H.E. Hackney, D.F. Perepichka, Recent advances in room temperature phosphorescence of crystalline boron containing organic compounds, Aggregate 3 (4) (2022);
e) Z. Xiao, N. Li, W. Yang, Z. Huang, X. Cao, T. Huang, Z. Chen, C. Yang, Saccharin-derived multifunctional emitters featuring concurrently room temperature phosphorescence, thermally activated delayed fluorescence and aggregation-induced enhanced emission, Chem. Eng. J. 419 (2021);
f) Q. Liu, M. Xie, X. Chang, S. Cao, C. Zou, W.F. Fu, C.M. Che, Y. Chen, W. Lu, Tunable multicolor phosphorescence of crystalline polymeric complex salts with metallophilic backbones, Angew. Chem. Int. Ed. 57 (21) (2018) 6279–6283;
g) J. Li, Z. Song, Y. Chen, C. Xu, S. Li, Q. Peng, G. Shi, C. Liu, S. Luo, F. Sun, Z. Zhao, Z. Chi, Y. Zhang, B. Xu, Colour-tunable dual-mode afterglows and helical-array-induced mechanoluminescence from AIE enantiomers: Effects of molecular arrangement on formation and decay of excited states, Chem. Eng. J. 418 (2021).

[6] a) N.J. Turro, J.D. Bolt, Y. Kuroda, I. Tabushi, A study of the kinetics of inclusion of halonaphthalenes with ß-cyclodextrin via time correlated phosphorescence, Photochem. Photobiol. 35 (1) (1982) 69–72, https://doi.org/10.1111/j.1751-1097.1982.tb03812.x;
b) L.F. Vieira Ferreira, I. Ferreira Machado, A.S. Oliveira, M.R. Vieira Ferreira, J. P. Da Silva, J.C. Moreira, A diffuse reflectance comparative study of benzil inclusion within p-tert- butylcalix[n]arenes (n = 4, 6, and 8) and silicalite, J. Phys. Chem. B. 106 (48) (2002) 12584–12593, https://doi.org/10.1021/jp021685n;
c) Z. Liu, W. Lin, Y. Liu, Macrocyclic supramolecular assemblies based on hyaluronic acid and their biological applications, Acc. Chem. Res. 55 (23) (2022) 3417–3429;
d) D. Li, F. Lu, J. Wang, W. Hu, X.-M. Cao, X. Ma, H. Tian, Amorphous metal-free room-temperature phosphorescent small molecules with multicolor photoluminescence via a host–guest and dual-emission strategy, J. Am. Chem. Soc. 140 (5) (2018) 1916–1923;
e) K. Wang, J.H. Jordan, K. Velmurugan, X. Tian, M. Zuo, X.Y. Hu, L. Wang, Role of functionalized pillararene architectures in supramolecular catalysis, Angew. Chem. Int. Ed. 60 (17) (2021) 9205–9214;
f) W.L. Zhou, Y. Chen, Q. Yu, H. Zhang, Z.-X. Liu, X.Y. Dai, J.J. Li, Y. Liu, Ultralong purely organic aqueous phosphorescence supramolecular polymer for targeted tumor cell imaging, Nat. Commun. 11 (1) (2020) 4655;
g) D. Li, Z. Liu, M. Fang, J. Yang, B.Z. Tang, Z. Li, Ultralong room-temperature phosphorescence with second-level lifetime in water based on cyclodextrin supramolecular assembly, ACS Nano 17 (13) (2023) 12895–12902.

[7] a) L. Kong, Y. Zhu, S. Sun, H. Li, S. Dong, F. Li, F. Tao, L. Wang, G. Li, Tunable ultralong multicolor and near-infrared emission from polyacrylic acid-based room temperature phosphorescence materials by FRET, Chem. Eng. J. 469 (2023), 143931, https://doi.org/10.1016/j.cej.2023.143931;
b) H. Louis, M. Thomas, A. Gmelch, F. Haft, S. Fries, Reineke, Blue-light-absorbing thin films showing ultralong room-temperature phosphorescence, Adv. Mater. 31 (12) (2019) 1807887. https://doi.org/10.1002/adma.201807887;
c) Y. Zhou, L. Jin, J. Chen, W. Hong, G. Liang, W. Qin, Five-in-one: Dual-mode ultralong persistent luminescence with multiple responses from amorphous polymer films, Chem. Eng. J. 463 (2023), 142506. https://doi.org/10.1016/j.cej.2023.142506;
d) S. Hirata, K. Totani, J. Zhang, T. Yamashita, H. Kaji, S.R. Marder, T. Watanabe, C. Adachi, Efficient persistent room temperature phosphorescence in organic amorphous materials under ambient conditions, Adv. Funct. Mater. 23 (27) (2013) 3386–3397. https://doi.org/10.1002/adfm.201203706;
e) X. Zheng, J. Jiang, Q. Lin, C. Li, J. Chen, S. Wang, Q. Han, X. Ye, Y. Liu, X. Tao, Excitation- & concentration-dependent color-tunable ultra-long phosphorescence

of isophthalonitriles doped polymers, Chem. Eng. J. 469 (2023), 143929. https://doi.org/10.1016/j.cej.2023.143929;
f) X. Yang, Y. Dong, S. Ma, J. Ren, N. Li, S. Lü, Humidity-resistant organic room-temperature phosphorescence materials synthesized using catalyst-free click reaction, Chem. Eng. J. 462 (2023), 142198. https://doi.org/10.1016/j.cej.2023.142198.

[8] X. Yao, J. Wang, D. Jiao, Z. Huang, O. Mhirsi, F. Lossada, L. Chen, B. Haehnle, A.J. C. Kuehne, X. Ma, H. Tian, A. Walther, Room-temperature phosphorescence enabled through nacre-mimetic nanocomposite design, Adv. Mater. 33 (5) (2021) 2005973, https://doi.org/10.1002/adma.202005973.

[9] a) L. Gu, H. Wu, H. Ma, W. Ye, W. Jia, H. Wang, H. Chen, N. Zhang, D. Wang, C. Qian, Z. An, W. Huang, Y. Zhao, Color-tunable ultralong organic room temperature phosphorescence from a multicomponent copolymer, Nat. Commun. 11 (1) (2020) 944, https://doi.org/10.1038/s41467-020-14792-1;
b) Y. Su, Y. Zhang, Z. Wang, W. Gao, P. Jia, D. Zhang, C. Yang, Y. Li, Y. Zhao, Excitation-dependent long-life luminescent polymeric systems under ambient conditions, Angew. Chem. Int. Ed. 59 (25) (2020) 9967–9971. https://doi.org/10.1002/anie.201912102;
c) Y. Yang, K.Z. Wang, D. Yan, Smart luminescent coordination polymers toward multimode logic gates: Time-resolved, tribochromic and excitation-dependent fluorescence/phosphorescence emission, ACS Appl. Mater. Interfaces. 9 (20) (2017) 17399–17407. https://doi.org/10.1021/acsami.7b00594.

[10] R. Ferreira, C. Baleizão, J.M. Muñoz-Molina, M.N. Berberan-Santos, U. Pischel, Photophysical study of bis(naphthalimide)-amine conjugates: Toward molecular design of excimer emission switching, J. Phys. Chem. A 115 (6) (2011) 1092–1099, https://doi.org/10.1021/jp110470h.

[11] a) T.C. Barros, G.R. Molinari, P. Berci Filho, V.G. Toscano, M.J. Politi, Photophysical properties of N-alkylnaphthalimides and analogs, J. Photoch. Photobio. A. 76(1-2) (1993) 55-60. https://doi.org/10.1016/1010-6030(93)80173-7; b) T.C. Barros, P.B. Filho, V.G. Toscano, M.J. Politi, Intramolecular excimer formation from 1,8-n-alkyldinaphthalimides, J. Photoch. Photobio. A. 89 (2) (1995) 141-146. https://doi.org/10.1016/1010-6030(95)04040-M.

[12] D.W. Cho, D.W. Cho, Excimer and exciplex emissions of 1,8-naphthalimides caused by aggregation in extremely polar or nonpolar solvents, New J. Chem. 38 (6) (2014) 2233–2236, https://doi.org/10.1039/C3NJ01473H.

[13] a) X. Chen, C. Xu, T. Wang, C. Zhou, J. Du, Z. Wang, H. Xu, T. Xie, G. Bi, J. Jiang, X. Zhang, J.N. Demas, C.O. Trindle, Y. Luo, G. Zhang, Versatile room-temperature-phosphorescent materials prepared from n-substituted naphthalimides: Emission enhancement and chemical conjugation, Angew. Chem. Int. Ed. 55 (34) (2016) 9872–9876, https://doi.org/10.1002/anie.201601252;
b) B. Ventura, A. Bertocco, D. Braga, L. Catalano, S. d'Agostino, F. Grepioni, P. Taddei, Luminescence properties of 1,8-naphthalimide derivatives in solution, in their crystals, and in co-crystals: Toward room-temperature phosphorescence from organic materials, J. Phys. Chem. c. 118 (32) (2014) 18646–18658. https://doi.org/10.1021/jp5049309.

[14] F.F. Shen, Y. Chen, X. Xu, H.J. Yu, H. Wang, Y. Liu, Supramolecular assembly with near-infrared emission for two-photon mitochondrial targeted imaging, Small 17 (30) (2021) 2101185, https://doi.org/10.1002/smll.202101185.

[15] J. Xu, H. Feng, H. Teng, G. Chen, S. Pan, J. Chen, Z. Qian, Reversible switching between phosphorescence and fluorescence in a unimolecular system controlled by external stimuli, Chem. Eur. J. 24 (49) (2018) 12773–12778, https://doi.org/10.1002/chem.201801739.

[16] W. Zhang, B. Wu, S. Sun, P. Wu, Skin-like mechanoresponsive self-healing ionic elastomer from supramolecular zwitterionic network, Nat. Commun. 12 (1) (2021) 4082, https://doi.org/10.1038/s41467-021-24382-4.

[17] A.T. Tarekegne, J. Janting, H. Ou, Strong visible-light emission in annealed poly (acrylic acid), Opt. Mater. Express. 10 (12) (2020) 3424–3434, https://doi.org/10.1364/OME.411329.

[18] J. Zhang, W. Wang, Y. Zhang, Q. Wei, F. Han, S. Dong, D. Liu, S. Zhang, Small-molecule ionic liquid-based adhesive with strong room-temperature adhesion promoted by electrostatic interaction, Nat. Commun. 13 (1) (2022) 5214, https://doi.org/10.1038/s41467-022-32997-4.

[19] I. Noda, Generalized two-dimensional correlation method applicable to infrared, raman, and other types of spectroscopy, Appl. Spectrosc. 47 (9) (1993) 1329–1336, https://doi.org/10.1366/0003702934067694.

[20] a) F. Ni, N. Qiu, P. Xiao, C. Zhang, Y. Jian, Y. Liang, W. Xie, L. Yan, T. Chen, Tillandsia-inspired hygroscopic photothermal organogels for efficient atmospheric water harvesting, Angew. Chem. Int. Ed. 59 (43) (2020) 19237–19246, https://doi.org/10.1002/anie.202007885;
b) S. Wu, H. Shi, S. Wei, H. Shang, W. Xie, X. Chen, W. Lu, T. Chen, Bio-inspired electro-thermal-hygro responsive rewritable systems with temporal/spatial control for environment-interactive information display, Small 19 (24) (2023) 2300191. https://doi.org/10.1002/smll.202300191.

[21] S. Wei, W. Lu, H. Shi, S. Wu, X. Le, G. Yin, Q. Liu, T. Chen, Light-writing & projecting multicolor fluorescent hydrogels for on-demand information display, Adv. Mater. 35 (25) (2023) 2300615, https://doi.org/10.1002/adma.202300615.